INTERNATIONAL JOURNAL FOR NUMERICAL METHODS IN ENGINEERING
Int. J. Numer. Meth. Engng 2010; **83**:575–597
Published online 9 March 2010 in Wiley InterScience (www.interscience.wiley.com). DOI: 10.1002/nme.2844

A data-driven stochastic collocation approach for uncertainty quantification in MEMS

Nitin Agarwal and N. R. Aluru*, †

Department of Mechanical Science and Engineering, Beckman Institute for Advanced Science and Technology, University of Illinois at Urbana-Champaign, 405 N. Mathews Avenue, Urbana, IL 61801, U.S.A.

SUMMARY

This work presents a data-driven stochastic collocation approach to include the effect of uncertain design parameters during complex multi-physics simulation of Micro-ElectroMechanical Systems (MEMS). The proposed framework comprises of two key steps: first, probabilistic characterization of the input uncertain parameters based on available experimental information, and second, propagation of these uncertainties through the predictive model to relevant quantities of interest. The uncertain input parameters are modeled as independent random variables, for which the distributions are estimated based on available experimental observations, using a nonparametric diffusion-mixing-based estimator, Botev (Nonparametric density estimation via diffusion mixing. *Technical Report*, 2007). The diffusion-based estimator derives from the analogy between the kernel density estimation (KDE) procedure and the heat dissipation equation and constructs density estimates that are smooth and asymptotically consistent. The diffusion model allows for the incorporation of the prior density and leads to an improved density estimate, in comparison with the standard KDE approach, as demonstrated through several numerical examples. Following the characterization step, the uncertainties are propagated to the output variables using the stochastic collocation approach, based on sparse grid interpolation, Smolyak (*Soviet Math. Dokl.* 1963; **4**:240–243). The developed framework is used to study the effect of variations in Young's modulus, induced as a result of variations in manufacturing process parameters or heterogeneous measurements on the performance of a MEMS switch.

Received 28 August 2009; Accepted 2 December 2009

KEY WORDS: uncertainty quantification; nonparametric density estimation; diffusion estimator; stochastic collocation; Smolyak algorithm; sparse grids; polysilicon Young's modulus

*Correspondence to: N. R. Aluru, Department of Mechanical Science and Engineering, Beckman Institute for Advanced Science and Technology, University of Illinois at Urbana-Champaign, 405 N. Mathews Avenue, Urbana, IL 61801, U.S.A.
†E-mail: aluru@illinois.edu

Contract/grant sponsor: National Science Foundation; contract/grant number: 0601479
Contract/grant sponsor: DARPA/MTO
Contract/grant sponsor: DOE

1. INTRODUCTION

The rapid increase in the available computational power and an easier access to high-performance computing resources has enabled researchers to include the effect of underlying fluctuations or variations, while developing reliable predictive models for physical phenomenon. As a result, it is now possible to investigate the effect of uncertainties in various design parameters, such as material properties and geometrical features during the complex multi-physics simulation of Micro-ElectroMechanical Systems (MEMS), based on high-fidelity computational models. For MEMS, significant uncertainties in these design parameters are unavoidable due to a variety of factors such as low cost manufacturing processes, residual stresses, irregular surface topography and chemical contamination, etc. [1]. These uncertainties are described using stochastic quantities—uncertain parameters can be modeled as random variables and uncertain spatial or temporal functions can be represented as random fields or processes. Using this, the original governing equations are reformulated as stochastic partial differential equations (SPDEs). Recently, much of the research effort has focussed on developing numerical techniques to efficiently solve these SPDEs, which offer much improved performance as compared with the traditionally used sampling-based approaches such as Monte Carlo (MC) method (for an overview, see [2] and references therein). The most widely used methods include the stochastic Galerkin approach based on polynomial chaos (PC) expansion [3] and its generalizations [4–6]. Also, there has been a growing interest in another class of methods known as stochastic collocation method [7–11], which approximates the unknown stochastic solution using sparse grid interpolation in the multi-dimensional random domain, based on the Smolyak algorithm [12]. The stochastic collocation approach has emerged as an attractive alternative to the widely used Galerkin approach, as it offers high resolution similar to the Galerkin method, as well as ease of implementation as the sampling-based methods. We developed a stochastic Lagrangian framework (based on generalized PC) [13, 14], and an adaptive stochastic collocation approach [9, 15] for quantifying the effect of uncertainties in material properties and geometrical parameters on the performance of MEMS devices.

Any numerical solution procedure for stochastic systems, as a first step, requires characterization of input uncertain parameters in terms of random variables or fields. The choice of methodology and the ability to correctly characterize uncertain parameters largely depends on the extent of available experimental information regarding these parameters. This problem of generating stochastic models based on limited experimental data has been widely researched in various engineering and scientific disciplines, such as machine learning, data mining, computer vision, statistical mechanics etc. However, in the context of stochastic modeling of engineering systems, this particular aspect has remained relatively understated. Several researchers have employed the Karhunen-Loève (KL) expansion [16] to represent the random input parameters, modeled as random fields, in terms of a set of *uncorrelated* random variables (e.g. [17, 18]). This approach requires prior knowledge regarding the covariance function of the random field. PC expansion can also be used to represent random fields [19–21], where the coefficients of the PC modes can be determined based on the principles of maximum likelihood [20] or maximum entropy (MaxEnt) [21]. An information-theoretic framework based on the principle of maximum entropy has been used in [22], in the context of stochastic material modeling, in order to assign distributions to input parameters modeled as random variables. Although, these approaches provide attractive alternatives to infer stochastic models from experimental evidence and are based on sound theoretical ideas, they require information such as the covariance function (for KL-expansion), or the moments (for MaxEnt principle) for the uncertain parameters. Unfortunately, for MEMS, such detailed experimental observations

DOI: 10.1002/nme

for design variables, such as sufficient measurements for Young's modulus or gap between electrodes at various spatial locations, are not available. For most of the parameters, only limited observations (hundreds or less) may be available, given the associated difficulties with their experimental measurement. It is for this reason, that we propose to model the input parameters as a set of mutually independent random variables and estimate their distribution using *nonparametric density estimation techniques*.

In this work, we employ a *diffusion-mixing-based estimator* [23], in order to assign distributions to the uncertain input parameters modeled as mutually independent random variables, for which only very limited experimental information may be available. The diffusion based estimator derives from the analogy between the *kernel density estimation* (*KDE*) procedure, which is the most widely used nonparametric density estimation technique, and the heat dissipation equation [24]. As for the KDE technique, the diffusion model constructs smooth density estimates that are asymptotically consistent. In addition, it allows for the incorporation of the prior information regarding the uncertain parameters, in the density estimation procedure, within a non-Bayesian framework. In the absence of any prior information, the diffusion model leads to an improved density estimate, as compared with the standard KDE approach, which is demonstrated through several numerical examples. Following the characterization step, we employ the stochastic collocation approach [9, 15] to *propagate* the effect of these uncertainties to the output variables or the quantities of interest. Finally, the developed framework is used to study the effect of variations in Young's modulus, induced as a result of variations in manufacturing process parameters or heterogeneous measurements, on the performance of a MEMS switch.

The rest of the paper is organized as follows: In Section 2 we present the deterministic and stochastic formulation for the coupled electromechanical problem, applicable to static analysis of electrostatic MEMS. In Section 3 we discuss the density estimation procedure using both standard KDE and the diffusion-mixing-based approaches. We then briefly introduce the stochastic collocation framework used for uncertainty propagation in Section 4. In Section 5 we consider the numerical example of a MEMS switch and study the effect of uncertain parameters on its actuation behavior. We finally conclude the discussion in Section 6.

2. PROBLEM FORMULATION

2.1. Deterministic formulation—physical models

Physical level analysis of electrostatic MEMS requires a self-consistent solution of the coupled mechanical and electrostatic equations. A framework for the deterministic analysis is presented in [25], which uses a Lagrangian description both for the mechanical and the electrostatic domains. The mechanical deformation of the MEM structures is obtained by performing a 2-D geometrically nonlinear elasticity analysis [26]. Let Ω represent the undeformed configuration with boundary $d\Omega = d\Omega_g \cup d\Omega_h$. The governing equations for the deformation of the MEM structures in the absence of body force are given as

$$\nabla \cdot (\mathbf{FS}) = 0 \quad \text{in } \Omega, \tag{1}$$

$$\mathbf{u} = \mathbf{G} \quad \text{on } d\Omega_g, \tag{2}$$

$$\mathbf{P} \cdot \mathbf{N} = \mathbf{H} \quad \text{on } d\Omega_h, \tag{3}$$

DOI: 10.1002/nme

where **u** is the displacement vector, **F** is the deformation gradient, **P** and **S** are the first and second Piola–Kirchoff stress tensors, respectively. **H** is the electrostatic pressure acting on the surface of the structures and **N** is the unit outward normal vector in the undeformed configuration. The prescribed displacement is given by **G**. The constitutive law can be written as

$$\mathbf{S} = \mathscr{C}\mathbf{E}, \quad \mathbf{E} = \tfrac{1}{2}(\mathbf{F}^{\mathrm{T}}\mathbf{F} - \mathbf{I}), \tag{4}$$

where $\mathscr{C}$ is the material tensor and **E** is the Green–Lagrangian strain.

An electrostatic analysis is required to compute the electrostatic pressure acting on the surface of the microstructures. In the absence of any free charges, the electrostatic potential can be obtained by solving the Laplace equation, given as

$$\frac{\partial^2 \phi}{\partial x^2} + \frac{\partial^2 \phi}{\partial y^2} = 0 \quad \text{in } \bar{\omega}, \tag{5}$$

where ϕ is the potential field in the dielectric medium $\bar{\omega}$ (in the deformed configuration), surrounding the conductors. A Lagrangian boundary integral formulation (see [27] for details) of Equation (5) is used to compute the surface charge density $\sigma(\mathbf{X})$ on the conductors. The electrostatic pressure acting on the conductors in the undeformed configuration can be computed from the surface charge density as

$$\mathbf{H} = P_e J \mathbf{F}^{-\mathrm{T}} \mathbf{N}, \tag{6}$$

where $P_e = \sigma^2/2\varepsilon$ is the electrostatic pressure acting normal to the surface of the conductors and $J = \det(\mathbf{F})$. We can represent the deterministic coupled electromechanical system (Equations (1)–(3), (5) and (6)) as

$$\mathscr{L}(\mathbf{u}, \sigma; \mathbf{x}, \boldsymbol{\alpha}) = 0, \quad \mathbf{x} \in \Omega, \tag{7}$$

where $\boldsymbol{\alpha}$ represents the set of input parameters such as material properties—Young's modulus and the Poisson ratio, and various geometrical parameters, such as the dimensions of the electrodes or the gap between electrodes, etc. Given the values for the input parameters, such a system can be solved easily using finite element method (FEM) and boundary element method (BEM) [25, 28]. State-of-the-art design methodologies for MEMS are based on such deterministic approaches where the geometrical and physical properties of the device are assumed to be known precisely. However, in practice, such devices may be subjected to severe stochastic variations in these parameters, which must be considered during modeling.

2.2. *Stochastic formulation*

Let $(\Theta, B, \mathscr{P})$ denote a probability space, where Θ is the set of all possible values that $\boldsymbol{\alpha}$ can take (elementary events), B is the σ-algebra of events and $\mathscr{P}$ is the probability measure, which defines the probability of occurrence of a particular subset in the σ-algebra. The symbol θ specifies an elementary event in Θ and in the following presentation any quantity with θ-dependence denotes a random quantity. From the deterministic version of $\boldsymbol{\alpha}$ we now have a probabilistic definition of $\boldsymbol{\alpha}(\theta)$, which lies in the abstract probability space $(\Theta, B, \mathscr{P})$. Following this, the original governing equations (Equation (7)) are transformed as: we seek displacement $\mathbf{u}(\mathbf{x}, \boldsymbol{\alpha}(\theta)) : \bar{\Omega} \times \Theta \to \mathbb{R}$ and

DOI: 10.1002/nme

surface charge density $\sigma(\mathbf{x}, \boldsymbol{\alpha}(\theta)) : d\Omega \times \Theta \to \mathbb{R}$, such that for $\mathscr{P}$—almost everywhere $\theta \in \Theta$, the following holds

$$\mathscr{L}(\mathbf{u}, \sigma; \mathbf{x}, \boldsymbol{\alpha}(\theta)) = 0, \quad (\mathbf{x}, \theta) \in \Omega \times \Theta. \tag{8}$$

The numerical solution procedure for such a stochastic system comprises two key ingredients—first, we need to develop realistic stochastic models for uncertain input parameters, utilizing available experimental information and/or expert knowledge. Second, we seek to quantify the effect of variations in these input parameters on dependent variables, or in other words, *propagate* the uncertainty in the input variables to the dependent variables, in a computationally efficient manner. Specifically, we are interested in computing the moments—such as mean and variance, and the probability density function (PDF) of relevant quantities of interest. In next two sections, we present the computational framework for generating stochastic models for uncertain input parameters based on experimental information, and briefly discuss the stochastic collocation method for uncertainty propagation.

3. REPRESENTATION OF INPUT UNCERTAINTY

The first step towards numerical solution of Equation (8) is reducing the infinite dimensional probability space into a finite dimensional space, by representing the uncertain input parameters in terms of a finite number of random variables. The choice of methodology and the ability to correctly characterize uncertain parameters in terms of random variables largely depends on the extent of available experimental information regarding these parameters. For example, parameters for which sufficient measurements at various spatial locations are available, can be modeled as random fields. These random fields can then be expressed in terms of random variables using KL expansion [16–18] or PC expansion [19–21]. Unfortunately, for MEMS, such detailed experimental observations regarding important design parameters such as material properties and geometrical features are not available. Given limited experimental information, we model the input parameters $\boldsymbol{\alpha} = \{\alpha_i\}_{i=1}^n$ as a set of mutually independent random variables and estimate their distribution based on given observations.

We state the *density estimation problem* as follows: Given experimental observations $\{z_1, z_2, \ldots, z_M\}$ for a univariate random variable Z, we wish to estimate the unknown PDF $f(z)$. The density estimation problem has numerous applications and has been widely explored in various engineering and scientific disciplines. The methods available for density estimation can be broadly classified as parametric and nonparametric estimation. The parametric methods assume certain functional form of the distribution (e.g. uniform, normal, etc.) and simply seek to determine the parameters governing that functional form, based on some appropriate performance criterion. On the other hand, nonparametric methods are more general, as these methods do not assume any particular form *a priori*, but seek to construct the density estimates based on given data. The most widely used nonparametric density estimation technique is the kernel-based density estimation, and is considered next.

3.1. Kernel density estimation (KDE)

KDE techniques [29] have been widely used in various inference procedures in machine learning, data mining, pattern recognition, computer vision, etc. The KDE constructs an estimate $\hat{f}(z)$ for

DOI: 10.1002/nme

the unknown PDF $f(z)$ as

$$\hat{f}(z) = \frac{1}{M\beta} \sum_{i=1}^{M} K\left(\frac{z - z_i}{\beta}\right), \tag{9}$$

where $K(s)$ is the *kernel function*, β is the *bandwidth* and M represents the total number of given observations. The kernel $K(s)$ is required to satisfy the following two conditions:

$$K(s) \geqslant 0 \quad \text{and} \quad \int_{\mathbb{R}} K(s)\,\mathrm{d}s = 1. \tag{10}$$

The most widely used kernel is the Gaussian of zero mean and unit variance, using which, the KDE can be written as

$$\hat{f}(z) = \frac{1}{M\sqrt{2\pi\beta^2}} \sum_{i=1}^{M} \mathrm{e}^{-(z-z_i)^2/2\beta^2}, \tag{11}$$

which gives a smooth and asymptotically consistent density estimate.

The only unknown in Equation (11) is the bandwidth parameter β. Over the years, a lot of research have focused on the optimal choice of β, since the performance of $\hat{f}(z)$ as an estimator depends crucially on the choice of the bandwidth parameter [30]. One important consideration for various bandwidth selection methods is the choice of criterion for measuring the performance of the KDE estimates. One such widely used criterion is the mean integrated square error (MISE) given as,

$$\mathrm{MISE}(\beta) = \mathbb{E}\left[\int_{\mathbb{R}} (\hat{f}(z) - f(z))^2\,\mathrm{d}z\right], \tag{12}$$

where $\mathbb{E}[\cdot]$ refers to the average over various realizations of M observations. Several bandwidth selection methods seek to minimize the first-order asymptotic approximation of the MISE, known as AMISE, such as the Least Squares Cross-Validation [31], Biased Cross-Validation [32] and *solve-the-equation plug-in* method [33]. It can be shown that the bandwidth β^* chosen using the plug-in method reduces the AMISE at a rate $\mathcal{O}(M^{-4/5})$.

Another class of bandwidth selection methods, such as the Maximum-Likelihood Cross Validation (MLCV) method [34], employs the idea of likelihood to judge the quality of the density estimate. The rationale behind this method is to estimate the log-likelihood of the density at observation z_i based on all observations except z_i. Averaging this log-likelihood over all observations results in the following MLCV score:

$$\mathrm{MLCV}(\beta) = \frac{1}{M} \sum_{i=1}^{M} \log \hat{f}_{-i}(z_i), \tag{13}$$

where $\hat{f}_{-i}(z)$ denotes the density estimated from all the data points except z_i, and is known as the *leave-one estimator*. Using the estimator in Equation (11), the MLCV score can be rewritten as

$$\mathrm{MLCV}(\beta) = \frac{1}{M} \sum_{i=1}^{M} \log\left(\frac{1}{(M-1)\sqrt{2\pi\beta^2}} \sum_{j=1, j\neq i}^{M} \mathrm{e}^{-(z_i - z_j)^2/2\beta^2}\right). \tag{14}$$

DOI: 10.1002/nme

Following this, the optimal bandwidth β^* is chosen as

$$\beta^* = \arg\max_{\beta} \ \mathrm{MLCV}(\beta). \tag{15}$$

Since the MLCV method is based on the principle of maximum-likelihood, it has broader appeal and can be easily extended to more general choice of kernels (other than the Gaussian kernel), as is the case for the diffusion-mixing-based estimator, considered next.

3.2. Diffusion model for density estimation

We now present the diffusion-mixing-based estimator [23], which exploits the analogy between the KDE technique and the heat dissipation equation, to construct a powerful nonparametric density estimation procedure.

3.2.1. Diffusion interpretation of the Gaussian KDE. We first demonstrate the analogy between the KDE technique and the heat dissipation equation, as noted by Chaudhuri and Marron [24]. Consider the following heat diffusion equation:

$$\frac{\partial}{\partial t}\hat{f}(z,t) = \frac{1}{2}\frac{\partial^2}{\partial z^2}\hat{f}(z,t), \quad z \in \mathbb{R}, \quad t>0, \tag{16}$$

with initial and boundary conditions given as,

$$\hat{f}(z,0) = g(z), \quad z \in \mathbb{R} \quad \text{and} \quad \hat{f}(z,t) \to 0 \quad \text{as } z \to \pm\infty, \tag{17}$$

respectively, where $g(z)$ is the specified initial condition. The analytical solution of the heat diffusion equation can be written as (see [35]):

$$\hat{f}(z,t) = \frac{1}{\sqrt{2\pi t}} \int_{-\infty}^{\infty} g(s) \mathrm{e}^{-(z-s)^2/2t} \, \mathrm{d}s. \tag{18}$$

For the given observations $\{z_1, z_2, \ldots, z_M\}$, we can represent the empirical density $\Delta(z)$ as

$$\Delta(z) = \frac{1}{M}\sum_{i=1}^{M} \delta(z - z_i), \tag{19}$$

where $\delta(\cdot)$ represents the Dirac-delta function. For the initial condition $g(z) = \Delta(z)$, the solution of the heat equation takes the form

$$\hat{f}(z,t) = \frac{1}{\sqrt{2\pi t}} \int_{-\infty}^{\infty} \frac{1}{M}\sum_{i=1}^{M} \delta(z - z_i) \mathrm{e}^{-(z-s)^2/2t} \, \mathrm{d}s = \frac{1}{M\sqrt{2\pi t}} \sum_{i=1}^{M} \mathrm{e}^{-(z-z_i)^2/2t}. \tag{20}$$

This solution can be immediately recognized as the Gaussian KDE estimate (given by Equation (11)) with $\sqrt{t}$ playing the role of the bandwidth. This implies that finding the optimal bandwidth β^* of the KDE is equivalent to finding the optimal mixing time, denoted as t^*, of the diffusion process, initialized with the empirical density, and governed by Equation (16).

DOI: 10.1002/nme

3.2.2. Generalized diffusion model. We now consider the case where in addition to the experimental observations $\{z_1, \ldots, z_M\}$, we also have some prior information available for the scalar random variable Z. The prior information refers to the probability distribution $p(z)$ that expresses one's knowledge about the uncertain parameter, even before the experimental observations are taken into account, and is often based on purely subjective evaluation. For example, for the case when Z represents some geometrical parameter for a MEMS device, such as the gap between the electrodes, a reasonable choice for the prior distribution would be to use the Gaussian distribution with mean equal to the nominal (or desired) gap value, with variance selected based on the manufacturing tolerances. In such situations, the analogy between the Gaussian KDE and the diffusion model can be further exploited to incorporate the available prior information, leading to the generalized diffusion model (see [23] for details), given as

$$\frac{\partial}{\partial t}\hat{f}(z,t) = \frac{1}{2}\frac{\partial}{\partial z}\left(a(z)\frac{\partial}{\partial z}\left(\frac{\hat{f}(z,t)}{p(z)}\right)\right), \quad z \in \mathscr{H}, \quad t>0, \tag{21}$$

where $\mathscr{H}$ defines the computational domain, which can be set to be sufficiently large based on the range of given data and $a(z)$ is an arbitrary positive function on $\mathscr{H}$. We set $\hat{f}(z,t)=0$ at the boundaries of $\mathscr{H}$, and the initial condition is given as $\hat{f}(z,0)=\Delta(z)$. It must be noted that the solution of the PDE given by Equation (21) is a density $\hat{f}(z,t)$ such that,

- at time $t=0$, the density $\hat{f}(z,0)$ is same as the empirical density $\Delta(z)$ of the given experimental data;
- in the limit as $t \to \infty$ the density $\hat{f}(z,t)$ converges to the prior density, and,
- we can find an optimal mixing time $t^* \in (0,\infty)$, which mixes the prior density $p(z)$ with the empirical density $\Delta(z)$, in such a way that it maximizes the MLCV score.

As explained in [23] we can employ the heat dissipation analogy to develop an intuitive understanding about the statistical properties of the solution of the generalized diffusion model (Equation (21)). We can think of each empirical observation as a point temperature source, then $\Delta(z)$ is an initial temperature profile, while the PDE (Equation (21)) models its dissipation in a medium with variable diffusivity. In addition to variable diffusivity, the generalized diffusion model also provides a drift component for any non-constant $a(z)$ (such that $a'(z) \neq 0$). The nonuniform diffusivity and drift depend on the prior density $p(z)$ in such a way that in regions where we expect more observations (i.e. higher prior density), the empirical data tend to get dissipated slower (lesser smoothing) and drifts less. On the other hand, in regions where we expect fewer observations (i.e. lower prior density), the empirical data dissipate faster (more smoothing) and drift more towards regions of high density (data sharpening). Thus, the generalized diffusion model allows for variable smoothing and data sharpening in different regions, which makes it a more powerful nonparametric density estimation model in cases where we have prior information.

For cases where we have no prior information, we can use a two-stage estimation procedure for improved accuracy as follows:

- Stage 1: Given experimental observations, we employ the standard Gaussian KDE (Equation (11)) to obtain the estimate $\hat{f}_0(z)$, where the optimal bandwidth β^* is chosen according to the maximum likelihood criterion, Equation (15). The estimate $\hat{f}_0(z)$ is known as the *pilot estimate*.

DOI: 10.1002/nme

Table I. Test problems for comparison of standard KDE and generalized diffusion model.

S. no.	Name	Target density $f(z)$
1	Strongly skewed density	$\sum_{k=0}^{7} \frac{1}{8}\mathcal{N}(3((\frac{2}{3})^k-1),(\frac{2}{3})^{2k})$
2	Kurtotic unimodal density	$\frac{2}{3}\mathcal{N}(0,1)+\frac{1}{3}\mathcal{N}(0,(\frac{1}{10})^2)$
3	Claw density	$\frac{1}{2}\mathcal{N}(0,1)+\sum_{k=0}^{4}\frac{1}{10}\mathcal{N}(\frac{k}{2}-1,(\frac{1}{10})^2)$

- Stage 2: Given the experimental observations and the pilot estimate $\hat{f}_0(z)$, we solve the generalized diffusion equation (Equation (21)) with $p(z)=\hat{f}_0(z)$ and $a(z)=(\hat{f}_0(z))^\gamma$, $\gamma\in[0,1]$, to obtain the final density estimate $\hat{f}(z,t^*)$. The optimal mixing time t^* is chosen according to the maximum likelihood criterion, such that

$$t^*=\arg\max_t \ \mathrm{MLCV}(t), \quad \mathrm{MLCV}(t)=\frac{1}{M}\sum_{i=1}^{M}\log \hat{f}_{-i}(z_i,t), \tag{22}$$

  where $\hat{f}_{-i}(z,t)$ is the *leave-one* estimator obtained as the solution of the PDE (Equation (21)) with initial condition $\hat{f}(z,0)=\Delta_{-i}(z)=(1/(M-1))\sum_{j=1,j\neq i}^{M}\delta(z-z_j)$.

As noted in [23], various modifications of the standard KDE that have been presented in the literature, can be seen as special cases of the generalized diffusion model. For example, the choice of $p(z)=\hat{f}_0(z)$ and $a(z)=(\hat{f}_0(z))^\gamma$, $\gamma\in[0,1]$ leads to a KDE based on Gaussian kernels with variable mean and bandwidth, as proposed in [36].

One may argue that the computation of the leave-one estimators in stage 2 may be computationally expensive, as it involves repeated solution of the PDE given by Equation (21). However, since we propose to use the diffusion model to improve accuracy in situations where very limited experimental information may be available, the computational cost would not be that significant. Moreover, in any case, the overall computational cost of the density estimation step would be insignificant in comparison with the uncertainty propagation step, as that involves thousands of expensive simulations of the coupled electromechanical system.

3.2.3. Numerical examples. We now consider several test problems to demonstrate that the two-stage estimator based on generalized diffusion model leads to improved accuracy, especially for cases where the target densities may be complex, for which only limited experimental information may be available. The test problems are listed in Table I, where $\mathcal{N}(\mu,v^2)$ refers to the Gaussian distribution with mean μ and variance v^2. These standard test problems have been taken from [23, 37].

In order to asses the quality of the density estimates $\hat{f}(z)$, we compute the MISE, which is obtained by averaging the integrated square error (ISE) $=\int_{\mathbb{R}}[\hat{f}(z)-f(z)]^2\,\mathrm{d}z$ over 10 independent simulations. In Figures 1–3 we plot the MISE for the density estimates obtained using standard KDE and the generalized diffusion model (for $\gamma=0.0, 0.5$ and 1.0) using various sample sizes for the test problems 1–3, as listed in Table I. As can be clearly seen, the diffusion model significantly improves the accuracy as compared with the classical KDE procedure. We must note that for the choice $\gamma=1.0$, $p(z)=a(z)=\hat{f}_0(z)$, which implies using uniform diffusivity and variable drift in the generalized diffusion model. Such a choice would only provide data sharpening, and is

DOI: 10.1002/nme

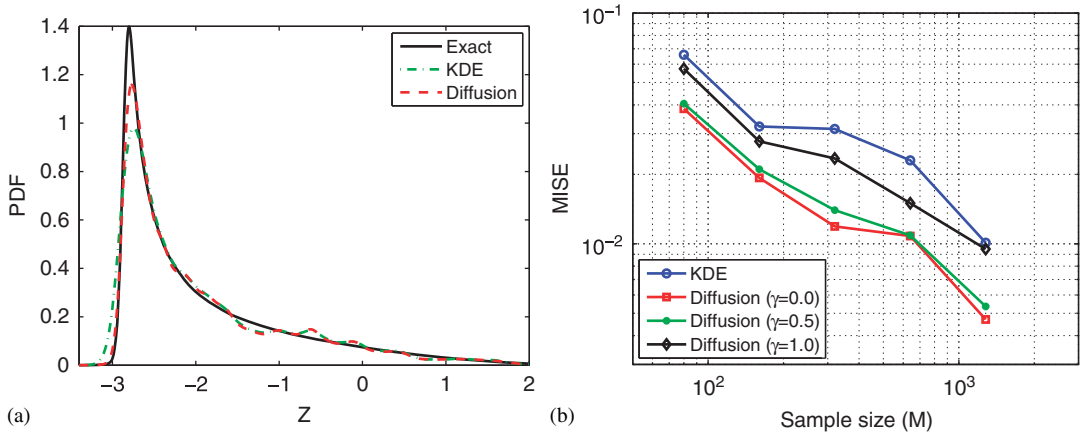

Figure 1. Comparison of density estimates obtained using standard KDE and diffusion model for strongly skewed target density. (a) Target density and density estimates for $M = 400$; $\gamma = 0.5$ and (b) mean integrated square error (MISE).

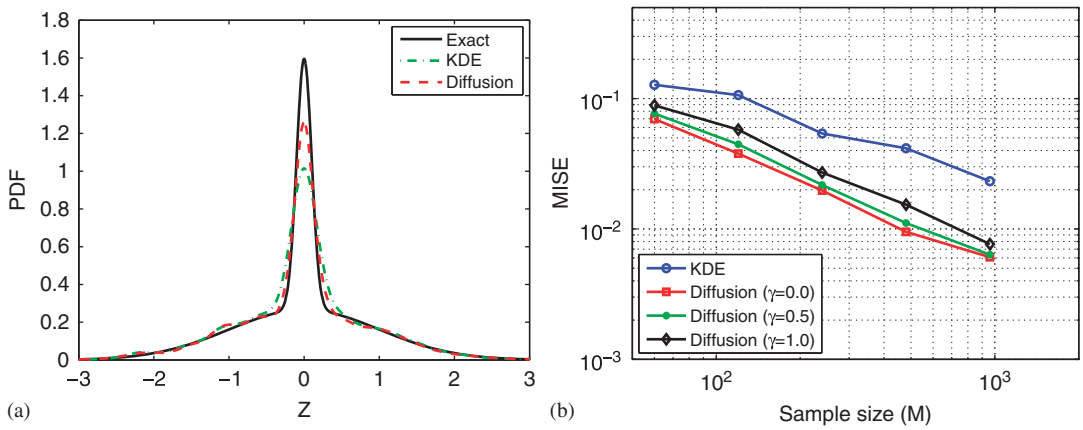

Figure 2. Comparison of density estimates obtained using standard KDE and diffusion model for kurtotic unimodal target density. (a) Target density and density estimates for $M = 300$; $\gamma = 0.5$ and (b) mean integrated square error (MISE).

asymptotically equivalent to using KDE based on Gaussian kernels with variable mean and uniform bandwidth [23]. For other choices of $0<\gamma<1$, the diffusion model offers both variable diffusivity as well as drift, leading to more improvement over the standard KDE approach as compared with the choice $\gamma=1.0$, as can be seen from Figures 1–3. For examples presented in later sections, we have used $\gamma=0.5$.

In addition, we also compare the density estimates obtained using the two approaches with the exact target densities. As can be seen from Figures 1(a)–3(a), the diffusion model better predicts the high density peaks (for all test cases), as well as the low density valleys (for the claw density example). This improvement is the result of the variable smoothing and data sharpening in various regions, offered by the generalized diffusion model. In Figure 4 we illustrate the selection of

DOI: 10.1002/nme

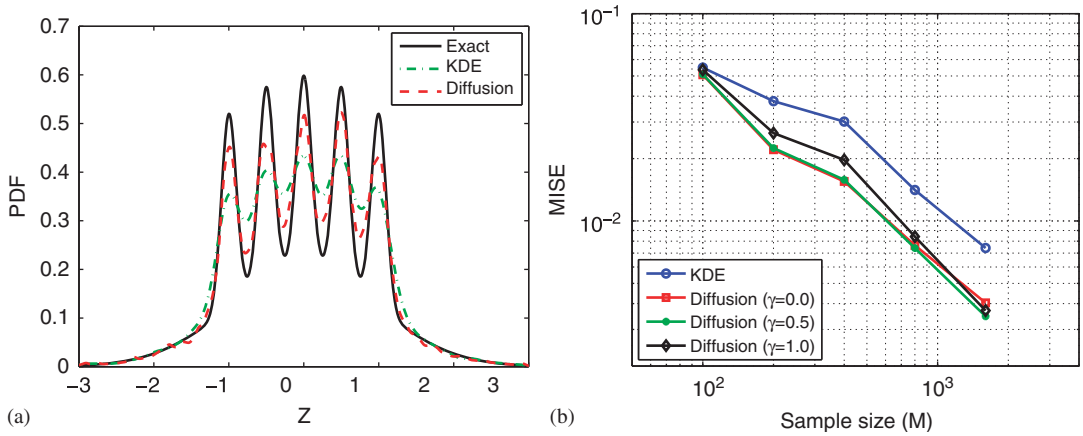

Figure 3. Comparison of density estimates obtained using standard KDE and diffusion model for claw target density. (a) Target density and density estimates for $M = 400$; $\gamma = 0.5$ and (b) mean integrated square error (MISE).

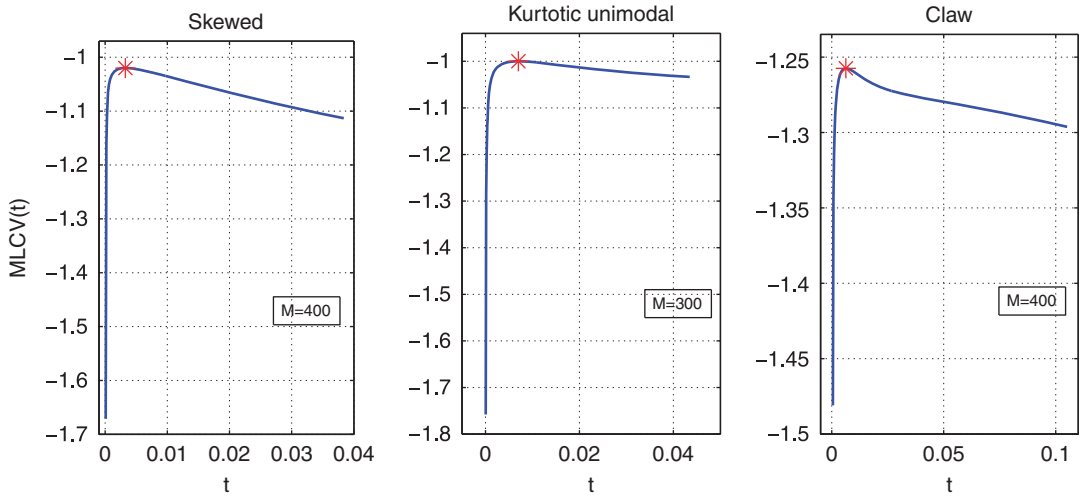

Figure 4. Illustration of selection of optimal mixing time t^* based on the MLCV cost function for various target densities.

optimal mixing time t^* for the considered target densities, based on the maximum-likelihood cost function MLCV(t), using one particular realization of M observations for each case.

4. UNCERTAINTY PROPAGATION

Having characterized input uncertain parameters in terms of random variables (with known distribution), we now seek to quantify the effect of variations in these parameters on dependent variables.

DOI: 10.1002/nme

We are interested in computing the moments—such as mean and variance, and the PDF of relevant quantities of interest.

The characterization of uncertain input parameters $\boldsymbol{\alpha}(\theta)$ as independent random variables leads to reformulation of the stochastic coupled electromechanical problem (given by Equation (8)) as follows: we first define $\boldsymbol{\xi}=\{\xi_i\}_{i=1}^n$ as the set of mutually independent random variables with images $\Gamma_i=[0,1]$ and PDFs $\rho_i:\Gamma_i\to\mathbb{R}^+$, that map onto the set of input random parameters $\boldsymbol{\alpha}=\{\alpha_i\}_{i=1}^N$ with PDFs $f_i:\mathscr{H}_i\to\mathbb{R}^+$, for $i=1,\ldots,n$. The joint PDF $\rho(\boldsymbol{\xi})$ can be written as

$$\rho(\boldsymbol{\xi})=\prod_{i=1}^{n}\rho_i(\xi_i)\quad\forall\boldsymbol{\xi}\in\Gamma, \tag{23}$$

where $\Gamma=\prod_{i=1}^n\Gamma_i=[0,1]^n$ represents the support of the set of random variables. Using this, we can rewrite Equation (8) as: we seek random displacement $\mathbf{u}(\mathbf{x},\boldsymbol{\xi})$ and surface charge density $\sigma(\mathbf{x},\boldsymbol{\xi})$, such that

$$\mathscr{L}(\mathbf{u},\sigma;\mathbf{x},\boldsymbol{\xi})=0,\quad(\mathbf{x},\boldsymbol{\xi})\in\Omega\times\Gamma, \tag{24}$$

which represents a $(d+n)$-dimensional system, where d and n refer to the dimensionality of the physical space Ω and the random space Γ, respectively.

4.1. Stochastic collocation method

Traditionally, sampling-based methods, such as MC method, have been used for systems with random input parameters. Such statistical methods involve generating various realizations of the input parameters according to the underlying probability distribution, and repeatedly employing the deterministic solver for each realization. Although the MC method is highly scalable (as its convergence does not depend on n) and straightforward to implement, it offers slow convergence rate. Thus, for complex multi-physics MEMS problems, based on high-fidelity computational models, it often becomes impractical due to prohibitive computational cost. Recently, there has been a growing interest in another class of methods known as stochastic collocation method [7–11, 38]. In [15] we presented a stochastic collocation-based framework for MEMS, assuming that the stochastic models for the input uncertain parameters are already provided. Here, we briefly introduce the stochastic collocation method based on sparse grid interpolation (see [7–11, 13–15] for details).

The basic idea of the stochastic collocation approach is to approximate the unknown stochastic solution by a polynomial interpolation function in the multi-dimensional random space. The interpolation is constructed using the sparse grid interpolation technique, which involves solving (sampling) the deterministic problem at a *pre-determined* set of points $\Theta_N=\{\boldsymbol{\xi}^i\}_{i=1}^N$. The set of nodes Θ_N are chosen as the sparse grid points generated using the Smolyak algorithm [12], unlike the MC approach where the sampling points are chosen in a statistical manner. At each of the sparse grid nodes $\{\boldsymbol{\xi}^i\}_{i=1}^N$, we solve the deterministic problem $\mathscr{L}(\mathbf{u},\sigma;\mathbf{X},\boldsymbol{\xi}^i)=0$ and obtain the field variables $[\mathbf{u}(\mathbf{X},\boldsymbol{\xi}^i),\sigma(\mathbf{X},\boldsymbol{\xi}^i)]$. Using these sampled values, the approximate displacement $\hat{\mathbf{u}}(\mathbf{X},\boldsymbol{\xi})$ and surface charge density $\hat{\sigma}(\mathbf{X},\boldsymbol{\xi})$ can be written as

$$\hat{\mathbf{u}}(\mathbf{X},\boldsymbol{\xi})=\sum_{i=1}^{N}\mathbf{u}(\mathbf{X},\boldsymbol{\xi}^i)L_i(\boldsymbol{\xi}),\quad\hat{\sigma}(\mathbf{X},\boldsymbol{\xi})=\sum_{i=1}^{N}\sigma(\mathbf{X},\boldsymbol{\xi}^i)L_i(\boldsymbol{\xi}), \tag{25}$$

DOI: 10.1002/nme

where $\{L_i(\boldsymbol{\xi})\}_{i=1}^{N}$ are the multi-dimensional interpolation basis functions, generated as special tensor products of the univariate basis functions, according to the Smolyak algorithm. We note that, using the deterministic solution at a few collocation points, the entire stochastic solution can be constructed. For example, the deformation at any point $\boldsymbol{\xi} \in \Gamma$ in the random domain is simply given as $\hat{\mathbf{u}}(\mathbf{X}, \boldsymbol{\xi})$.

Using the sampled values for the unknown stochastic solution, we can compute the required moments in a straightforward manner. For example, the mth-moment of the random displacement $\mathbf{u}(\mathbf{X}, \boldsymbol{\xi})$ can be computed as

$$\mu_m(\mathbf{u})(\mathbf{X}) = \mathbb{E}[\mathbf{u}^m(\mathbf{X}, \boldsymbol{\xi})] = \int_{\Gamma} \mathbf{u}^m(\mathbf{X}, \boldsymbol{\xi}) \rho(\boldsymbol{\xi}) \, \mathrm{d}\boldsymbol{\xi} \tag{26}$$

$$= \sum_{i=1}^{N} \mathbf{u}^m(\mathbf{X}, \boldsymbol{\xi}^i) w_i, \quad w_i = \int_{\Gamma} \rho(\boldsymbol{\xi}) L_i(\boldsymbol{\xi}) \, \mathrm{d}\boldsymbol{\xi}, \tag{27}$$

where $\{w_i\}_{i=1}^{N}$ are the weights that can be pre-computed, using the estimated distribution $\rho(\boldsymbol{\xi})$ and prior knowledge of the basis functions. In addition, we can also generate the PDF for the output solution $\mathbf{u}(\mathbf{X}, \boldsymbol{\xi})$, by effectively using the constructed sparse grid interpolant. Given the distribution $\rho(\boldsymbol{\xi})$, we first generate N_{mh} (such that $N_{mh} \gg N$) samples $\{\boldsymbol{\xi}^i\}_{i=1}^{N_{mh}}$, using the Metropolis–Hastings algorithm [39] and then evaluate the interpolant in Equation (25) to obtain $\{\boldsymbol{u}(\mathbf{X}, \boldsymbol{\xi}^i)\}_{i=1}^{N_{mh}}$. These output values can then be used to construct a histogram, which following an appropriate normalization gives the PDF for the output.

Since the stochastic collocation approach only involves repeated application of the previously validated computational models (such as FEM-BEM model described in Section 2), the stochastic implementation is simply developed as a *wrapper* around the already existing deterministic code. Also, for the number of uncertain parameters that one usually needs to consider for the analysis of electrostatic MEMS, this approach has been shown to be orders of magnitude faster than the MC method [7]. Moreover, unlike MC method, based on the sampled values, this approach constructs an explicit representation of the dependent variables in terms of the input parameters, which can be effectively used for visualization or sensitivity analysis.

4.2. Numerical example

We now present a numerical example to demonstrate the two steps involved in the data-driven uncertainty quantification procedure, namely, density estimation based on experimental data, and uncertainty propagation. Specifically, we consider the function

$$g(\alpha_1, \alpha_2) = \cos(\pi\alpha_1)\cos(\pi\alpha_2), \tag{28}$$

where α_1 and α_2 are assumed to be mutually independent random variables, each distributed according to a bimodal distribution, such that

$$\alpha_i \sim \tfrac{1}{2}\mathcal{N}(5, 1) + \tfrac{1}{2}\mathcal{N}(0, (\tfrac{1}{5})^2), \quad i = 1, 2,$$

where $\mathcal{N}(\mu, v^2)$ refers to the Gaussian distribution with mean μ and variance v^2. We wish to quantify the error in moments of $g(\cdot, \cdot)$ (mean and variance), both due to the limited experimental information available, as well as the accuracy of the sparse grid interpolation used, as governed by the sample size M used for density estimation and the size of the sparse grid N, respectively.

DOI: 10.1002/nme

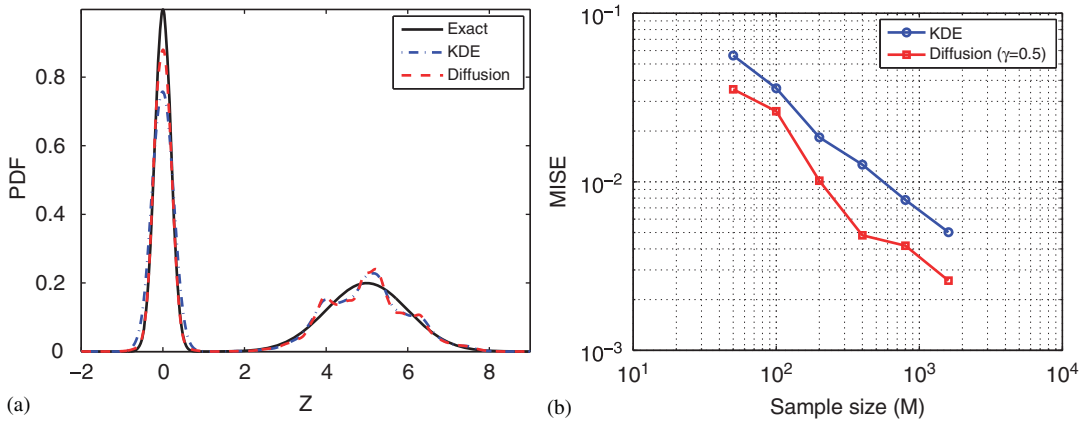

Figure 5. Comparison of density estimates for $\alpha_i, i=1,2$, obtained using standard KDE and diffusion model (using $\gamma=0.5$). (a) Target density and density estimates for M = 200 and (b) mean integrated square error (MISE).

In Figure 5(a) we first compare the density estimates obtained using standard KDE and the diffusion model (using $M=200$ observations) with exact density. As for the test cases considered earlier, the diffusion model better predicts the high density peak, as compared with the standard approach. This improvement in performance can be further verified from Figure 5(b), where we plot the MISE using both the approaches for various sample sizes M.

In Figure 6 we plot the error in mean and variance with increasing sparse grid size N, where the density is estimated based on standard KDE using two different sample sizes, $M=200$ and 1600. In addition, we also plot the error in moments obtained using the exact distribution for the input variables. We note that, using a sufficiently accurate sparse grid ($N=32769$) with exact densities for input variables leads to an accuracy in the range $\sim 10^{-6}$. However, using the same sparse grid with estimated densities based on $M=1600$ samples, the accuracy is only restricted to $\sim 10^{-2}$. This signifies that, while one can improve the accuracy of the uncertainty propagation step, the level of accuracy that can be achieved for the quantities of interest depends on the extent of available experimental information. This point is further demonstrated in Figure 7, where we plot the error in the moments for various sample sizes M, while using a sufficiently accurate sparse grid ($N=32769$). As can be seen, the density estimation procedure based on the diffusion model leads to a significant improvement in the accuracy of the moments, as compared with the standard KDE approach. The improved performance for the diffusion model can be attributed to the better prediction of high density peak, as shown in Figure 5(a).

5. NUMERICAL RESULTS: MEMS SWITCH

In this section, we employ the data-driven stochastic collocation framework to quantify the effect of uncertain design parameters such as material properties and geometrical parameters on the performance of MEMS devices. Specifically, we consider a micro-switch, modeled as a polysilicon cantilever beam which is 80 μm long, 1 μm thick and 10 μm wide, located over a ground plane at a distance g, as shown in Figure 8. We wish to quantify the effect of uncertainty in Young's modulus

DOI: 10.1002/nme

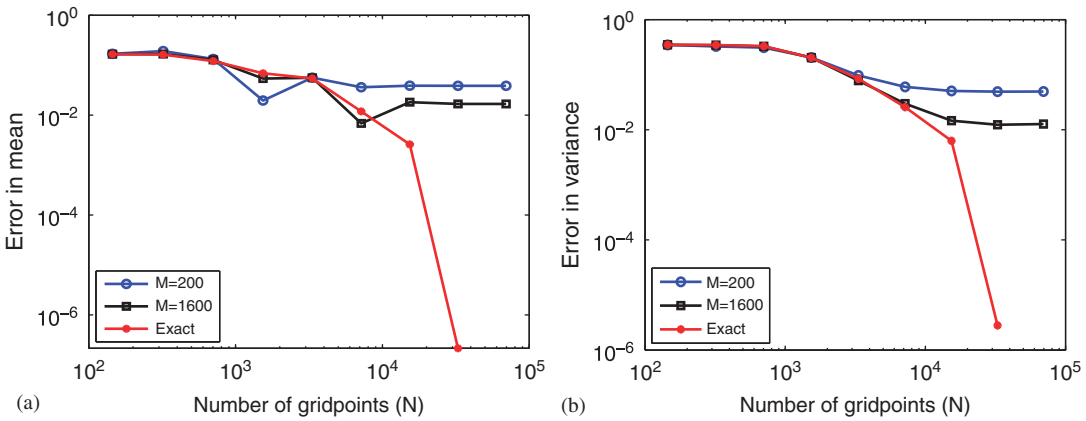

Figure 6. Error in moments for the test function for various sample sizes M and increasing sparse grid size N. (a) Error in mean and (b) error in variance.

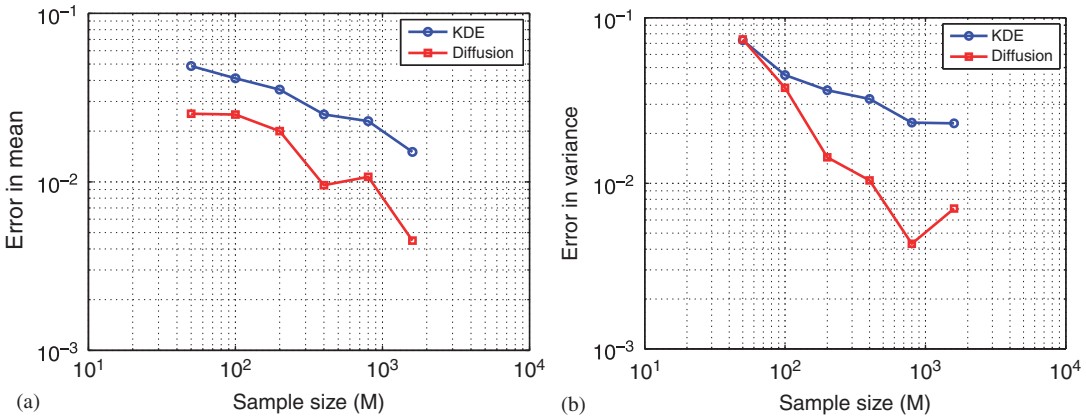

Figure 7. Error in the moments due to limited experimental information using standard KDE and diffusion model. (a) Error in mean and (b) error in variance.

of polysilicon E, and the gap between the electrodes g, on the vertical tip displacement of the switch. These two key design parameters for MEMS may be subjected to significant uncertainties due to a variety of factors, including the variations in the manufacturing process parameters or even lack of knowledge, owing to difficulties in experimental measurements.

5.1. Uniform vs skewed distribution

We first demonstrate the effect of the distribution of the input parameters on the performance of MEMS switch, by assuming that the two input parameters are modeled as follows:

$$E = E_0(1 + v_E(2\xi_1 - 1)) \quad \text{and} \quad g = g_0(1 + v_g(2\xi_2 - 1)), \tag{29}$$

DOI: 10.1002/nme

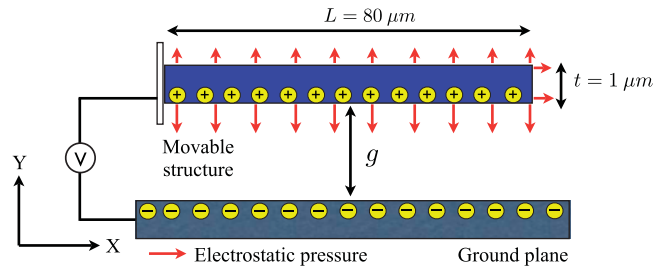

Figure 8. MEMS switch modeled as a deformable cantilever beam over a ground plane.

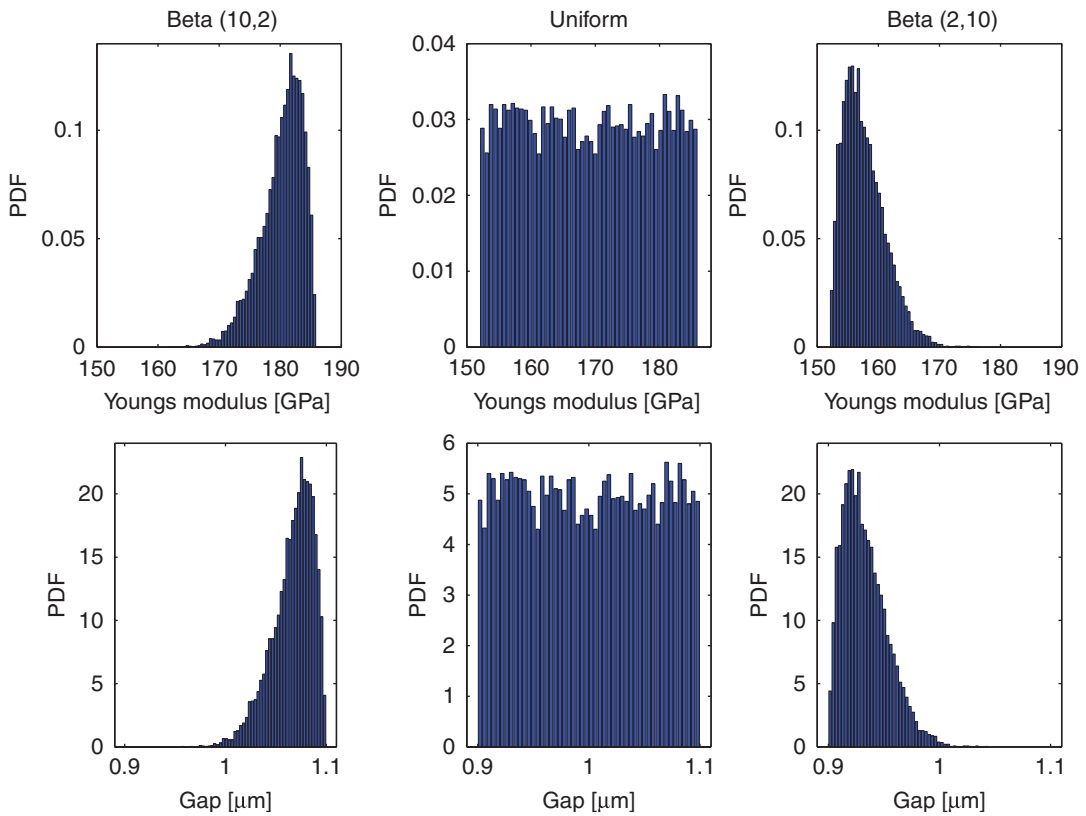

Figure 9. Assumed distributions for Young's modulus and gap between electrodes.

where $E_0 = 169\,\text{GPa}$, $g_0 = 1\,\mu\text{m}$, $v_E = v_g = 0.1$, and $\xi_{1,2}$ are i.i.d random variables in $[0, 1]$. We consider 3 cases, where ξ_1 and ξ_2 are assumed to be beta$(10, 2)$, uniform and beta$(2, 10)$ distributed, resulting in uniform and skewed distributions for Young's modulus and gap, as shown in Figure 9.

DOI: 10.1002/nme

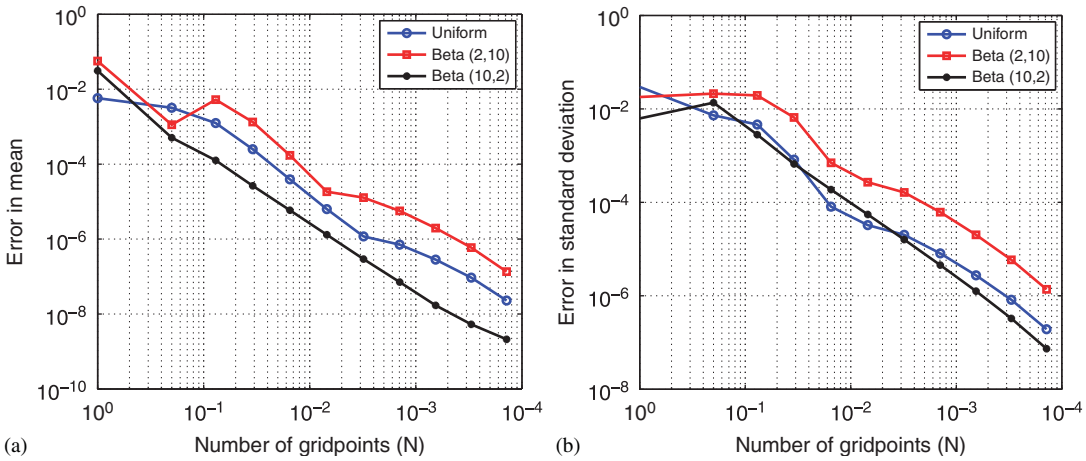

Figure 10. Error in moments of the vertical tip deflection with increasing sparse grid size N for assumed input distributions. (a) Error in mean and (b) error in standard deviation.

Using the stochastic collocation framework, we compute the mean and standard deviation for vertical tip deflection for various applied voltages $V \leqslant 7.0\,\mathrm{V}$. The mean and standard deviation values are obtained using a sufficiently accurate sparse grid with $N = 15\,361$, which results in an accuracy in the range $\sim \mathcal{O}(10^{-6})$, as shown in Figure 10. For the computation of error, as the actual moment values are not known, we treat the results using $N = 15\,361$ as *exact*, and report the maximum error for all applied voltages $V \leqslant 7.0\,\mathrm{V}$. As shown in Figure 11, the beta(2, 10) distribution results in higher mean deflection as compared with the other two cases, as it leads to Young's modulus and gap values skewed towards lower extremes. In addition, the uniform distribution leads to higher variability in the tip displacement, as compared with skewed beta distributions, as is evident from the higher standard deviation values. These observations underscore that in order to develop a stochastic modeling framework for MEMS which provides reliable results that can be validated, it is imperative to infer realistic stochastic models for the input parameters based on experimental data. We next consider the effect of variations in Young's modulus of polysilicon on the performance of MEMS switch, based on experimental data available in the literature.

5.2. *Effect of LPCVD process parameters*

Polysilicon films deposited by low pressure chemical vapor deposition (LPCVD) are the most widely used structural material for MEMS. However, the material properties of LPCVD polysilicon are known to vary significantly depending on the deposition conditions, such as temperature, doping and texture, as well as post-deposition processes. In [40] Lee *et al.* have presented extensive experimental results, investigating the effect of phosphorus doping and texture on Young's modulus of polysilicon films. Polysilicon films are deposited at temperatures of 585, 605 and 625°C, for varying phosphorous doping levels using $POCl_3$ and photosilicate glass as source. Young's modulus is obtained by taking the average of the values calculated from the resonant frequencies of four different sized lateral resonators.

We employ these experimental results to estimate the distribution for Young's modulus of polysilicon, and in turn, quantify the effect of variations in LPCVD process parameters on the

DOI: 10.1002/nme

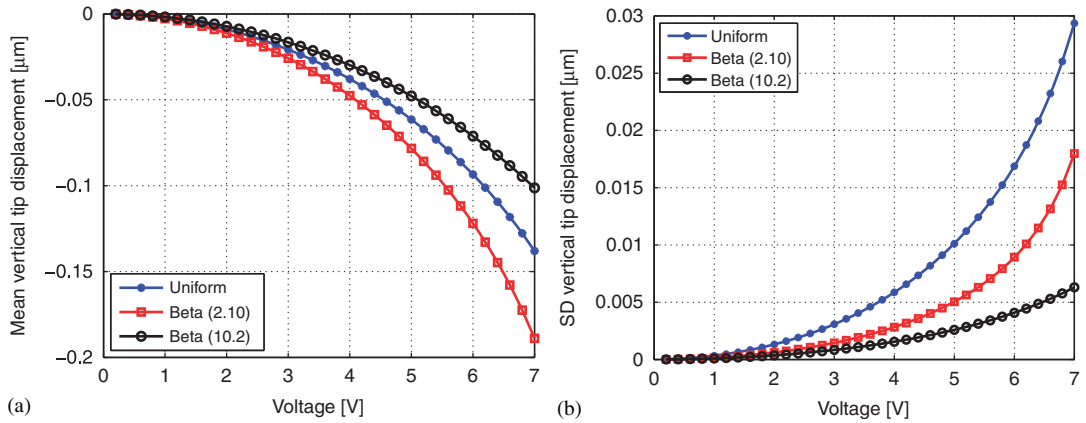

Figure 11. Effect of distribution of the input parameters on the output statistics for the MEMS switch. (a) Mean vertical tip deflection for various applied voltages V and (b) standard deviation of the vertical tip deflection for various applied voltages V.

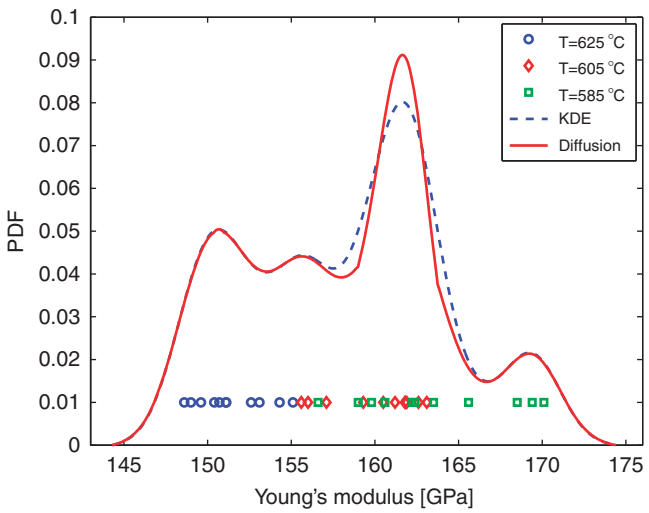

Figure 12. The density estimates and experimental observations ($M = 31$) [40] for Young's modulus of polysilicon films resulting from variability in the LPCVD process parameters.

performance of the MEMS switch considered earlier (Figure 8). We estimate the distribution for Young's modulus using both standard KDE and the diffusion model. The experimental observations as well as the estimated distribution using both approaches are shown in Figure 12. The diffusion model predicts a high density peak around 162 GPa, which seems to be consistent with the experimental data, as Young's modulus values for two different temperatures (605 and 585°C) are clustered in that region. For this study, as before, we assume that the gap g between the electrodes is uniformly distributed with mean $g_0 = 1\,\mu$m with 10% variation around the mean.

DOI: 10.1002/nme

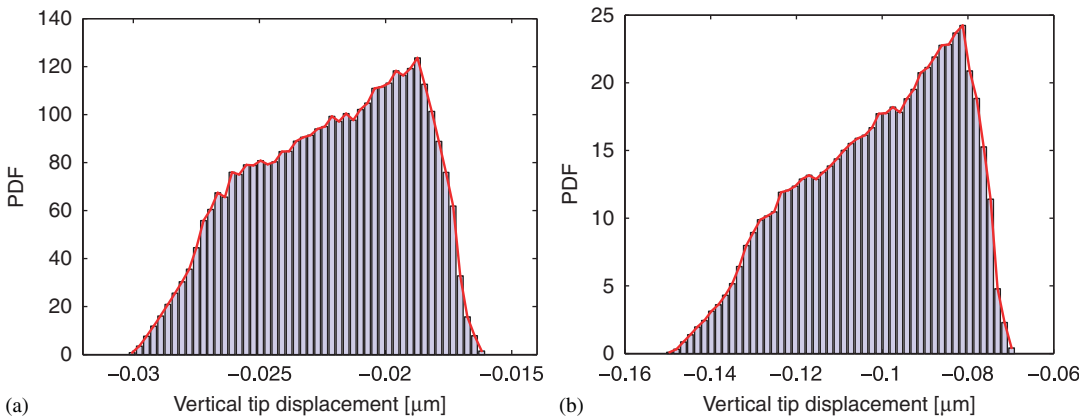

Figure 13. Effect of variability in the LPCVD process parameters on MEMS switch: probability density function (PDF) of vertical tip deflection for various applied voltages. (a) Applied voltage $V = 3.0\,\mathrm{V}$ and (b) applied voltage $V = 6.0\,\mathrm{V}$.

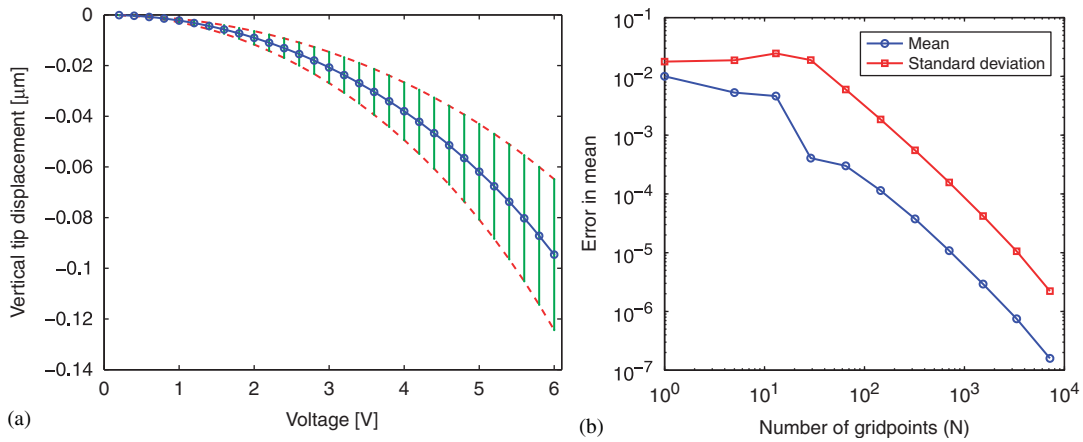

Figure 14. Statistics of the vertical tip displacement for MEMS switch. (a) Mean tip displacement with error bars based on standard deviation for various applied voltages V and (b) error in statistics with increasing sparse grid size N.

We employ the stochastic collocation framework to compute the moments and PDF of the vertical tip displacement for various applied voltages $V \leqslant 6\,\mathrm{V}$. The PDF of tip displacement for $V = 3.0\,\mathrm{V}$ and $6.0\,\mathrm{V}$ are shown in Figure 13. In Figure 14(a) we plot the mean vertical tip displacement with error bars based on standard deviation. The sparse grid interpolation employs sufficiently accurate grid with $N = 15\,361$, which leads to an accuracy in the range $\sim \mathcal{O}(10^{-7})$ for mean and $\sim \mathcal{O}(10^{-6})$ for standard deviation, as shown in Figure 14(b).

DOI: 10.1002/nme

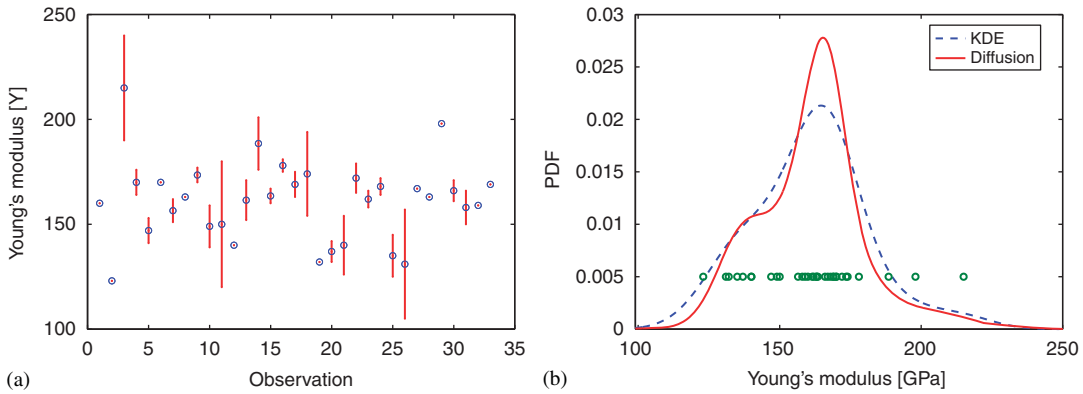

Figure 15. The density estimates and experimental observations ($M = 33$) [41] for Young's modulus of polysilicon films resulting from heterogeneous measurements. (a) Young's modulus values as measured by various researchers using different measuring techniques and (b) density estimates using standard KDE and diffusion model.

5.3. *Effect of heterogeneous measurements*

As polysilicon is the most widely used MEMS material, it is also the most widely tested. Over the years, various researchers have reported the material properties for polysilicon, based on various measuring techniques such as tension, bending, resonance, ultrasonic, indentation, etc. (as summarized in Table 3.5 in [41]). In addition to different measuring techniques being used, these results are based on tests performed on specimen, which may also differ in a variety of ways, based on the manufacturing process, specimen preparation technique, loading condition, residual stresses, etc. The probability distribution of Young's modulus inferred from such heterogeneous measurements provides valuable information, and in turn allows one to quantify the effect of uncertainty in a variety of factors on the performance of MEMS devices.

We plot the reported experimental values with their error bars (Figure 15(a)) and employ these to estimate the distribution of Young's modulus using standard KDE and diffusion model, as shown in Figure 15(b). Using the estimated distribution for Young's modulus and a uniform density for gap, we compute the PDF for the vertical tip displacement of the MEMS switch for $V = 3.0$ and 6.0 V, as shown in Figure 16. These plots indicate the variability induced in the tip displacement, as a result of lack of knowledge about Young's modulus and uncertainty in the gap between the electrodes.

6. CONCLUSIONS

This work presented a data-driven stochastic collocation approach which enables to include the effect of uncertain design variables, such as material properties and geometrical parameters during complex multi-physics simulation of MEMS. The stochastic modeling framework first characterizes the uncertain parameters in terms of independent random variables, based on available experimental evidence. Following the characterization step, the uncertainties in input parameters are then propagated through the predictive model to relevant quantities of interest using the stochastic

DOI: 10.1002/nme

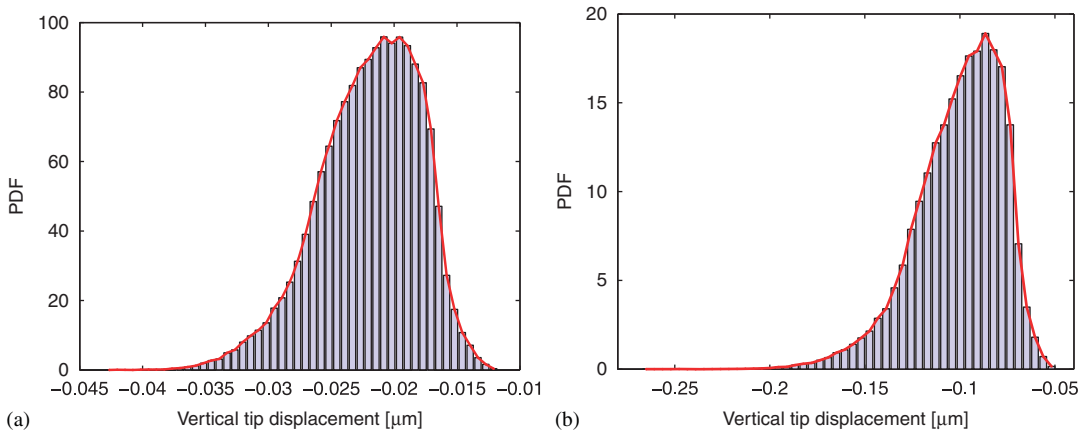

Figure 16. Effect of variability in input parameters on MEMS switch: probability density function (PDF) of vertical tip deflection for various applied voltages. (a) Applied voltage $V = 3.0\,\mathrm{V}$ and (b) applied voltage $V = 6.0\,\mathrm{V}$.

collocation approach. The density estimation procedure is based on a nonparametric diffusion-mixing-based estimator, which is derived using the analogy between KDE estimate and the heat dissipation equation. The diffusion model allows to incorporate any prior information that may be available regarding the uncertain parameters. In the absence of any prior information, a two-stage estimation procedure may be used, which leads to an improved density estimate, in comparison with the standard KDE procedure, as it allows for variable smoothing and data sharpening in different regions. Several numerical examples are presented to demonstrate that the diffusion model leads to significant improvement in the accuracy, especially for situations when complex target densities are estimated based on very limited experimental information. The stochastic collocation approach used for uncertainty propagation is based on sparse grid interpolation, and is known to provide faster convergence as compared with sampling-based methods, such as MC method, and is straightforward to implement. The developed framework is used to study the effect of variations in Young's modulus, induced as a result of variations in LPCVD process parameters or heterogeneous measurements, on the performance of a MEMS switch.

ACKNOWLEDGEMENTS

This work is supported by the National Science Foundation under grant number 0601479, by DARPA/MTO and by DOE.

REFERENCES

1. Liu M, Maute K, Frangopol DM. Multi-objective design optimization of electrostatically actuated microbeam resonators with and without parameter uncertainty. *Reliability Engineering and System Safety* 2007; **92**:1333–1343.
2. Xiu D. Fast numerical methods for stochastic computations: a review. *Communications in Computational Physics* 2009; **5**(2–4):242–272.
3. Ghanem RG, Spanos P. *Stochastic Finite Elements*: *A Spectral Approach*. Springer: Berlin, 1991.
4. Xiu D, Karniadakis GE. The Wiener–Askey polynomial chaos for stochastic differential equations. *SIAM Journal on Scientific Computing* 2002; **24**(2):619–644.

DOI: 10.1002/nme

5. Wan X, Karniadakis GE. An adaptive multi-element generalized polynomial chaos method for stochastic differential equations. *Journal of Computational Physics* 2005; **209**:617–642.
6. LeMâitre OP, Ghanem RG, Knio OM, Najm HN. Uncertainty propagation using Wiener–Haar expansions. *Journal of Computational Physics* 2004; **197**:28–57.
7. Xiu D, Hesthaven JS. High-order collocation methods for differential equations with random inputs. *SIAM Journal on Scientific Computing* 2005; **27**(3):1118–1139.
8. Ganapathysubramanian B, Zabaras N. Sparse grid collocation schemes for stochastic natural convection problems. *Journal of Computational Physics* 2007; **225**:652–685.
9. Agarwal N, Aluru NR. A domain adaptive stochastic collocation approach for analysis of MEMS under uncertainties. *Journal of Computational Physics* 2009; **228**(20):7662–7688.
10. Foo J, Wan X, Karniadakis GE. The multi-element probabilistic collocation method (ME-PCM): error analysis and applications. *Journal of Computational Physics* 2008; **227**(22):9572–9595.
11. Ma X, Zabaras N. An adaptive hierarchical sparse grid collocation algorithm for the solution of stochastic differential equations. *Journal of Computational Physics* 2009; **228**(8):3084–3113.
12. Smolyak S. Quadrature and interpolation formulas for tensor products of certain classes of functions. *Soviet Mathematics—Doklady* 1963; **4**:240–243.
13. Agarwal N, Aluru NR. A stochastic Lagrangian approach for geometrical uncertainties in electrostatics. *Journal of Computational Physics* 2007; **226**(1):156–179.
14. Agarwal N, Aluru NR. Stochastic modeling of coupled electromechanical interaction for uncertainty quantification in electrostatically actuated MEMS. *Computer Methods in Applied Mechanics and Engineering* 2008; **197**(43–44):3456–3471.
15. Agarwal N, Aluru NR. Stochastic analysis of electrostatic MEMS subjected to parameter variations. *Journal of Microelectromechanical Systems* 2009; **18**(6):1454–1468.
16. Loève M. *Probability Theory*. Springer: Berlin, 1977.
17. Babuska I, Liu K, Tempone R. Solving stochastic partial differential equations based on the experimental data. *Mathematical Models and Methods in Applied Sciences* 2003; **13**(3):415–444.
18. Ganapathysubramanian B, Zabaras N. A seamless approach towards stochastic modeling: sparse grid collocation and data-driven input models. *Finite Elements in Analysis and Design* 2008; **44**:298–320.
19. Ghanem R, Doostan A. On the construction and analysis of stochastic models: characterization and propagation of the errors associated with limited data. *Journal of Computational Physics* 2006; **217**:63–81.
20. Desceliers C, Ghanem R, Soize C. Maximum likelihood estimation of stochastic chaos representations from experimental data. *International Journal for Numerical Methods in Engineering* 2006; **66**:978–1001.
21. Das S, Ghanem R, Spall JC. Asymptotic sampling distributions for polynomial chaos representations from data: a maximum entropy and fisher information approach. *SIAM Journal on Scientific Computing* 2008; **30**(5):2207–2234.
22. Zabaras N, Sankaran S. An information-theoretic approach to stochastic materials modeling. *Computing in Science and Engineering* 2007; **9**(2):30–39.
23. Botev ZI. Nonparametric density estimation via diffusion mixing. *Technical Report*, The University of Queensland, 2007. Available from: http://espace.library.uq.edu.au/view/UQ:120006.
24. Chaudhuri P, Marron JS. Scale space view of curve estimation. *The Annals of Statistics* 2000; **28**(2):408–428.
25. De SK, Aluru NR. Full-Lagrangian schemes for dynamic analysis of electrostatic MEMS. *Journal of Microelectromechanical Systems* 2004; **13**(5):737–758.
26. Chandrasekharaiah DS, Debnath L. *Continuum Mechanics*. Academic: New York, 1994.
27. Li G, Aluru NR. A Lagrangian approach for electrostatic analysis of deformable conductors. *Journal of Microelectromechanical Systems* 2002; **11**:245–254.
28. Aluru NR, White J. An efficient numerical technique for electromechanical simulation of complicated microelectromechanical structures. *Sensors and Actuators A—Physical* 1997; **58**:1–11.
29. Wand MP, Jones MC. *Kernel Smoothing*. Chapman & Hall: London, 1995.
30. Jones MC, Marron JS, Sheather SJ. A brief survey of bandwidth selection for density estimation. *Journal of the American Statistical Association* 1996; **91**(433):401–407.
31. Bowman AW. An alternative method of cross-validation for the smoothing of density estimates. *Biometrika* 1984; **71**:353–360.
32. Scott DW, Terrell GR. Biased and unbiased cross-validation in density estimation. *Journal of the American Statistical Association* 1987; **82**:1131–1146.
33. Sheather SJ, Jones MC. A reliable data-based bandwidth selection method for kernel density estimation. *Journal of the Royal Statistical Society*, *Series B* 1991; **53**:683–690.

DOI: 10.1002/nme

34. Duin RPW. On the choice of smoothing parameters for Parzen estimators of probability density functions. *IEEE Transactions on Computers* 1976; **25**(11):1175–1179.
35. Strauss WA. *Partial Differential Equations*. Wiley: New York, 1992.
36. McKay IJ, Jones MC, Hu TC. Variable location and scale kernel density estimation. *Annals of the Institute of Statistical Mathematics* 1994; **46**:521–535.
37. Marron JS, Wand MP. Exact mean integrated error. *The Annals of Statistics* 1992; **20**:712–736.
38. Babuska I, Nobile F, Tempone R. A stochastic collocation method for elliptic partial differential equations with random input data. *SIAM Journal on Numerical Analysis* 2007; **45**(3):1005–1034.
39. Gilks W, Richardson S, Spiergelhalter D. *Markov Chain Monte Carlo in Practice*. Chapman & Hall: London, 1995.
40. Lee S, Cho C, Kim J, Park S, Yi S, Cho DD. The effect of post-deposition processes on polysilicon Young's modulus. *Journal of Micromechanics and Microengineering* 1998; **8**:330–337.
41. Sharpe WN. Mechanical properties of MEMS materials. *The MEMS Handbook*, Chapter 3, Gad-el-Hak M (ed.). CRC Press: Boca Raton, 2002.

DOI: 10.1002/nme